Concentric zones of active RhoA and Cdc42 around single cell wounds

Hélène A. Benink[1] and William M. Bement[1,2]

[1]Department of Zoology and [2]Program in Cellular and Molecular Biology, University of Wisconsin-Madison, Madison, WI 53706

Rho GTPases control many cytoskeleton-dependent processes, but how they regulate spatially distinct features of cytoskeletal function within a single cell is poorly understood. Here, we studied active RhoA and Cdc42 in wounded *Xenopus* oocytes, which assemble and close a dynamic ring of actin filaments (F-actin) and myosin-2 around wound sites. RhoA and Cdc42 are rapidly activated around wound sites in a calcium-dependent manner and segregate into distinct, concentric zones around the wound, with active Cdc42 in the approximate middle of the F-actin array and active RhoA on the interior of the array. These zones form before F-actin accumulation, and then move in concert with the closing array. Microtubules and F-actin are required for normal zone organization and dynamics, as is crosstalk between RhoA and Cdc42. Each of the zones makes distinct contributions to the organization and function of the actomyosin wound array. We propose that similar rho activity zones control related processes such as cytokinesis.

Introduction

One of the most fascinating and important features of cells is their ability to coordinate distinct motile activities in space and time in order to accomplish a particular task. Cell locomotion, for example, entails actin assembly at the leading edge integrated with myosin-based contraction toward the cell center and at the trailing edge (Lauffenburger and Horwitz, 1996). Similarly, coordinated interaction between actin assembly and actomyosin-based contraction is required for processes ranging from cytokinesis (Yumura and Uyeda, 2003) to morphogenesis (Jacinto et al., 2002). Consequently, understanding how such coordination is achieved is a subject of intense interest.

The rho GTPases—Rho, Rac, and Cdc42—are likely candidates to regulate spatially distinct aspects of actin-dependent motility (Ridley, 2001). Rac1 and Cdc42 control actin assembly via both overlapping and distinct targets (Bishop and Hall, 2000), whereas RhoA controls myosin-2–based contraction by promoting myosin-2 light chain phosphorylation via distinct targets (Kimura et al., 1996). Furthermore, now-classic studies have shown that, when activated, each of these proteins produces morphologically distinct, actin-based structures (Ridley, 2001). Moreover, the rho GTPases are themselves controlled by input from the microtubule cytoskeleton (Ren et al., 1999; Waterman-Storer and Salmon, 1999), which somehow coordinates actin assembly and actomyosin-based contraction during a variety of cellular motility processes (Rodriguez et al., 2003).

Other observations strongly support the notion that rho GTPases mediate spatial coordination of actomyosin-based assembly and contraction (Pertz and Hahn, 2004). Analyses of Rac1 and Cdc42 indicate that their active (i.e., GTP-bound) forms can be confined to discrete cellular regions (Kim et al., 2000; Kraynov et al., 2000; Sokac et al., 2003; Srinivasan et al., 2003; Nalbant et al., 2004). Furthermore, a recent study of the individual activation patterns of RhoA, Rac1, and Cdc42 suggests that each of the GTPases is activated in different regions during cell division (Yoshizaki et al., 2003). At present, however, simultaneous visualization of two distinct, active rho-class GTPases in single, living cells has not been achieved, nor has their differential distribution with respect to actin itself in living cells been reported. Thus, the extent to which rho GTPases control complex cellular motility processes via distinct patterns of distribution of their active forms is unclear.

Xenopus oocyte wound healing represents an ideal system in which to test potential spatial segregation of active rho GTPases. Wounding triggers rapid accumulation of actin filaments (F-actin) and myosin-2 around wounds as a result of both de novo assembly and actomyosin-based contraction (Mandato and Bement, 2001). Furthermore, the array of actomyosin around wounds segregates over time, with myosin-2

Correspondence to William M. Bement: wmbement@wisc.edu

Abbreviations used in this paper: 4D, time-lapse multiple focal plane; CARho, constitutively active RhoA; CACdc42, constitutively active Cdc42; DNCdc42, dominant negative Cdc42; MLC, myosin-2 regulatory light chain; mRFP, monomeric red fluorescent protein; ON, overnight; PM, plasma membrane; P-MLC, activated MLC; rGBD, the RhoA-binding domain of rhotekin; wGBD, the Cdc42-binding domain of N-WASP.

The online version of this article contains supplemental material.

The Journal of Cell Biology, Vol. 168, No. 3, January 31, 2005 429–439
http://www.jcb.org/cgi/doi/10.1083/jcb.200411109

concentrating on the interior of the array inside a broader zone of actin assembly (Bement et al., 1999; Mandato and Bement, 2001). Importantly, upstream regulators of actin polymerization and myosin-2 are recruited to wound edges after disruption of the F-actin cytoskeleton, which leads to the proposal that the zones of actin and myosin-2 assembly are themselves underlaid by local signaling zones established independently of F-actin. And, in keeping with findings from cell locomotion and cytokinesis, microtubule perturbation perturbs actin and myosin-2 recruitment during oocyte wound healing (Mandato and Bement, 2003).

Here, we assess the spatial and temporal patterns of active RhoA and Cdc42, the mechanisms that control their distribution, and their respective roles during oocyte wound healing. The results show that active RhoA and Cdc42 rapidly accumulate around wounds and segregate into distinct, dynamic "zones" that move inward as the actin array closes. Activity zone formation is dependent on calcium, and is controlled by inputs from the cortical actin cytoskeleton, microtubules, and crosstalk between the GTPases themselves. Furthermore, RhoA and Cdc42 make distinct contributions to the assembly, organization, and closure of the actomyosin array around wounds, consistent with their known roles.

Results

Concentric rings of rho GTPase activity around wounds

To visualize active RhoA, the RhoA-binding domain of rhotekin (rGBD) fused to either glutathione GST or eGFP was used; to visualize active Cdc42, the Cdc42-binding domain of N-WASP (wGBD) fused to either eGFP or monomeric red fluorescent protein (mRFP) was used (Campbell et al., 2002; Pertz and Hahn, 2004). rGBD binds specifically to active (GTP bound) RhoA in biochemical assays using cultured mammalian cells (Ren et al., 1999) or *Xenopus* brain extracts (Li et al., 2002), whereas wGBD binds specifically to active Cdc42 in *Xenopus* brain extracts (Li et al., 2002) and has previously been used to visualize active Cdc42 in mammalian cells (Kim et al., 2000) and *Xenopus* eggs (Sokac et al., 2003). The ability of these GBD probes to report endogenous rho GTPase activity was assessed by microinjection with the nonhydrolyzable GTP analogue GTP-γ-S or, as a control, water. Oocytes were then fixed and plasma membrane (PM) fluorescence was monitored directly (Fig. 1 A, eGFP) or by indirect immunofluorescence (Fig. 1, A and B, GST). GTP-γ-S more than doubled PM fluorescence relative to water in the presence of the GBD probes, whereas control oocytes injected with either GST or eGFP alone displayed little or no increase in PM fluorescence (Fig. 1, A and B). To further assess the GBD probes, PM GBD signal in oocytes microinjected with mRNA encoding constitutively active RhoA (CARho), constitutively active Cdc42 (CACdc42), dominant negative Cdc42 (DNCdc42), or C3 exotransferase (C3), a specific inhibitor of RhoA (Aktories et al., 2004), were compared with PM GBD levels in resting (i.e., unwounded) oocytes. CARho and CACdc42 significantly elevated levels of rGBD and wGBD fluorescence, respectively, at the PM, whereas C3 and DNCdc42 significantly reduced levels of rGBD and

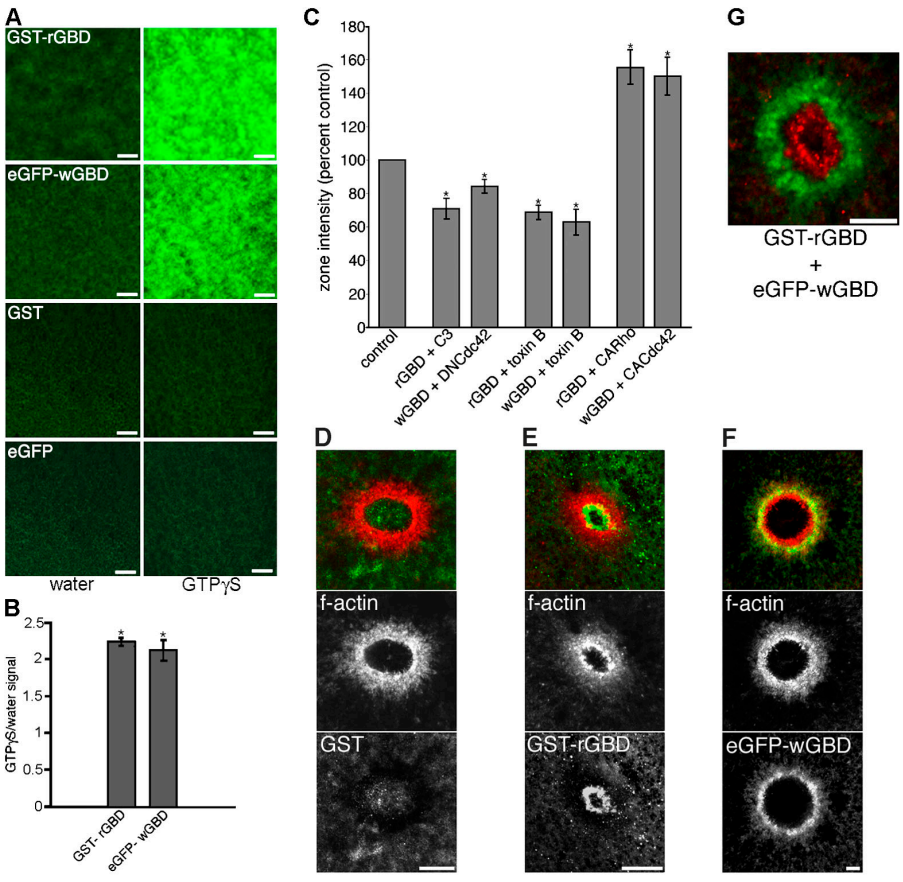

Figure 1. **Endogenous and exogenous rho GTPase activity in resting and wounded oocytes.** (A) Confocal images of plasma membrane (PM) fluorescence of oocytes injected with a GBD probe, GST, or eGFP, and subsequently injected with water or GTP-γ-S. Bars, 10 μm. (B) Quantification of PM fluorescence signal in oocytes containing the indicated probes and injected with water or GTP-γ-S ($n = 30$; results are shown as means ± SEM; asterisks indicate $P < 0.001$). (C) Quantification of background fluorescence intensity in resting oocytes containing the indicated probes and toxin B, C3 exotransferase (C3), or the specified construct, compared with controls containing the probes alone ($n \geq 3$; results are shown as means ± SEM; asterisks indicate $P < 0.001$). (D) Confocal images show lack of GST (green) localization around a wound relative to F-actin array (red). Bar, 10 μm. (E) Confocal images show ringlike localization of GST-rGBD (green) on interior of F-actin array (red). Bar, 10 μm. (F) Confocal images show ringlike colocalization of eGFP-wGBD (green) with F-actin array (red). Bar, 10 μm. (G) Confocal image shows zone of GST-rGBD (red) encircled by that of eGFP-wGBD (green). Bar, 10 μm.

wGBD, respectively (Fig. 1 C). Additionally, because wGBD has the potential to interact with N-WASP (Prehoda et al., 2000), oocytes were injected with Clostridium toxin B, which glycosylates and inactivates RhoA and Cdc42, but not proteins such as N-WASP, which lack the target glycosylation sites (Schirmer and Aktories, 2004). Toxin B reduced both rGBD and wGBD PM fluorescence (Fig. 1 C). Thus, the GBD reporters faithfully report the activation of both endogenous and exogenous RhoA and Cdc42 in resting oocytes. Further, as shown below, the GBD probes respond appropriately to manipulations designed to activate or inhibit RhoA and Cdc42 after wounding.

To assess the effects of wounding on RhoA and Cdc42 activity, oocytes were first injected with either GST-rGBD or eGFP-wGBD or, as controls, GST or eGFP, laser wounded, and then fixed and stained for the relevant probe and for F-actin, using fluorescent phalloidin. GST alone (Fig. 1 D) and eGFP alone (not depicted) did not localize around wounds. In contrast, the GBD probes displayed consistent and strikingly different patterns of distribution: GST-rGBD localized as a ring on the interior of the F-actin array, whereas eGFP-wGBD localized as a ring associated with the F-actin array (Fig. 1, E and F; and Fig. S1, A and B, available at http://www.jcb.org/cgi/content/full/jcb.200411109/DC1). To directly compare the distributions of active RhoA and Cdc42 around wounds in the same cell, we injected oocytes with both GST-rGBD and eGFP-wGBD, wounded them, and processed them for immunofluorescence. In these samples, GST-rGBD was concentrated in a ring that was circumscribed by a ring of eGFP-wGBD (Fig. 1 G), indicating that active Cdc42 and RhoA form concentric zones around wounds.

Dynamics of RhoA and Cdc42 activation around wounds

To characterize active GTPase dynamics, we injected oocytes with Alexa 568–actin and eGFP-rGBD or eGFP-wGBD and imaged them using time-lapse, multiple focal plane (4D) microscopy (Bement et al., 2003). Both zones of GTPase activity appeared ~20 s (rGBD, 18.7 ± 0.8 s; wGBD, 20.5 ± 0.9 s; n = 12) after wounding, significantly faster than actin accumulation (35.5 ± 0.9 s; n = 24, $P < 0.05$). However, each zone differed with respect to spatial dynamics. The RhoA activity zone was initially broad, extending up to ~30 μm from the wound border, but then rapidly narrowed from its outer edge inward (at 2.8 ± 0.1 μm/min; n = 3), until its peak signal was focused inside the

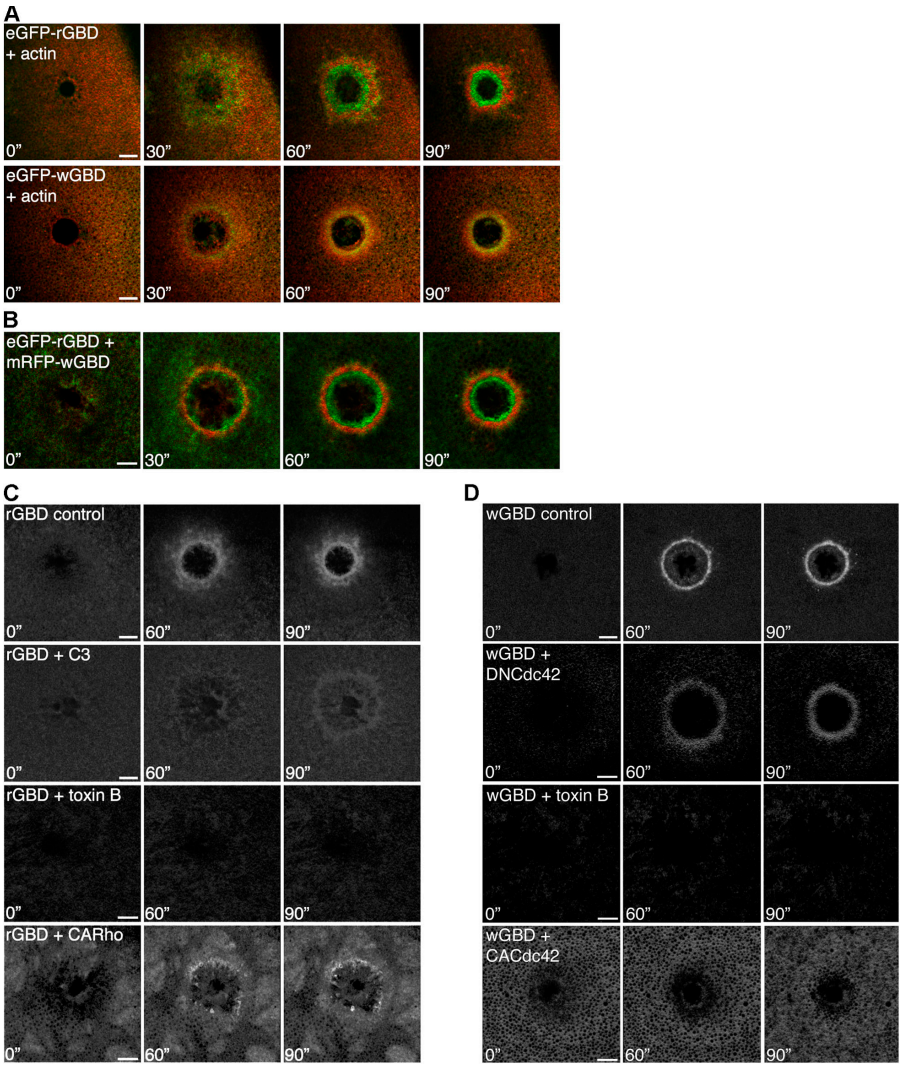

Figure 2. **Rho GTPase activity zone dynamics.** (A) Montage shows that zone of RhoA activity (eGFP-rGBD; green) appears as broad zone before focusing into a tight ring on actin array interior (red), whereas Cdc42 activity (eGFP-wGBD; green) appears and is maintained as a narrow zone in the middle of the actin array during wound healing (time in seconds; see Fig. S1). Bars, 15 μm. (B) Montage shows that RhoA (eGFP-rGBD; green) and Cdc42 (mRFP-wGBD; red) segregate into discrete zones during wound healing (time in seconds). Bar, 10 μm. (C) Montage shows that RhoA zone intensity (rGBD) is greatly reduced in the presence of C3 exotransferase (C3), toxin B, or constitutively active Rho (CARho), compared with control (time in seconds). Bars, 10 μm. (D) Montage shows that Cdc42 zone intensity of activity (wGBD) is greatly reduced in the presence of dominant negative Cdc42 (DNCdc42), toxin B, or constitutively active Cdc42 (CACdc42), compared with control (time in seconds). Bars, 10 μm. Videos available at http://www.jcb.org/cgi/content/full/jcb.200411109/DC1.

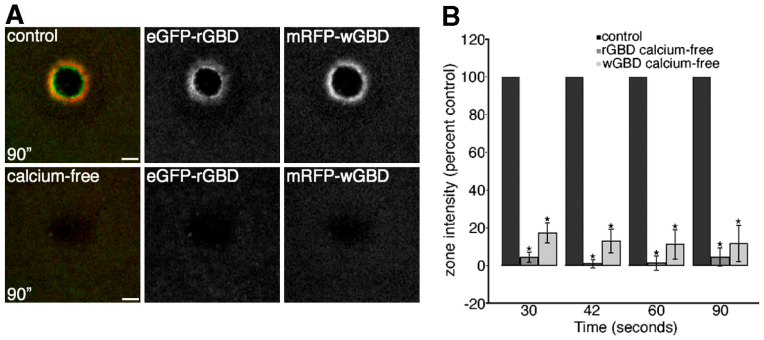

Figure 3. **External calcium is required for local activation of RhoA and Cdc42.** (A) Montage shows suppression of RhoA (eGFP-rGBD) and Cdc42 (mRFP-wGBD) activity zones at 90 s after wounding in calcium-free medium. Bars, 10 μm. (B) Quantification of GBD zone fluorescence intensity in the absence of external calcium, relative to controls, over time ($n = 11$; results are shown as means ± SEM; asterisks indicate $P < 0.001$).

actin array (Fig. 2 A, Videos 1 and 2, and Fig. S1 C). The zone of Cdc42 activity formed and was maintained as a 5–8-μm wide ring in the approximate middle of the actin array (Fig. 2 A, Videos 3 and 4, and Fig. S1 C). Once formed, both zones moved inward in concert with the actin array at ∼3–4 μm/min (rGBD, 3.4 ± 0.5 μm/min; wGBD 4.0 ± 0.6 μm/min; $n = 22$; Fig. 2 A and Videos 1 and 3). In addition to the narrow zone of Cdc42 activity distal from the wound edge observed in all wounds, in some wounds, active Cdc42 appeared in association with circular structures around the outside of the wound (Fig. 2 D, wGBD control), and, transiently, in a region near the wound border immediately after wounding (see Fig. 4 A, wGBD control).

To directly visualize the segregation of RhoA and Cdc42 activity zones in living cells, we microinjected oocytes with eGFP-rGBD and mRFP-wGBD. The dynamic patterns obtained using mRFP-wGBD and eGFP-rGBD were virtually identical to those observed using the individual GBD probes with AX-568 actin (Fig. 2 B and Video 5). Segregation of the two zones into concentric rings consistently occurred ∼60 s after wounding (60.5 ± 1.1; $n = 11$).

Oocytes were then wounded after being microinjected with C3, DNCdc42, toxin B, CARho, or CACdc42. C3 and DNCdc42 significantly reduced eGFP-rGBD and eGFP-wGBD recruitment, respectively, and toxin B completely eliminated both (Fig. 2, C and D). CARho and CACdc42, although they elevated background (resting) levels of RhoA and Cdc42 activity, apparently did so at the expense of activity zone formation around wounds. That is, CARho slowed and reduced recruitment of rGBD to wound borders, and CACdc42 almost completely eliminated wGBD recruitment (Fig. 2, C and D). Thus, perturbations that target RhoA and Cdc42 perturb the wound-induced accumulation of rGBD and wGBD, respectively, which is consistent with the rGBD and wGBD probes faithfully reporting the distribution of their intended targets. In addition, direct comparison of mRFP-wGBD to eGFP-Cdc42 shows that the latter is recruited to wounds (Fig. S2, available at http://www.jcb.org/cgi/content/full/jcb.200411109/DC1), which further supports the notion that the wGBD probe reports the distribution of Cdc42 rather than some other protein. We cannot, however, rule out the possibility that other mem-

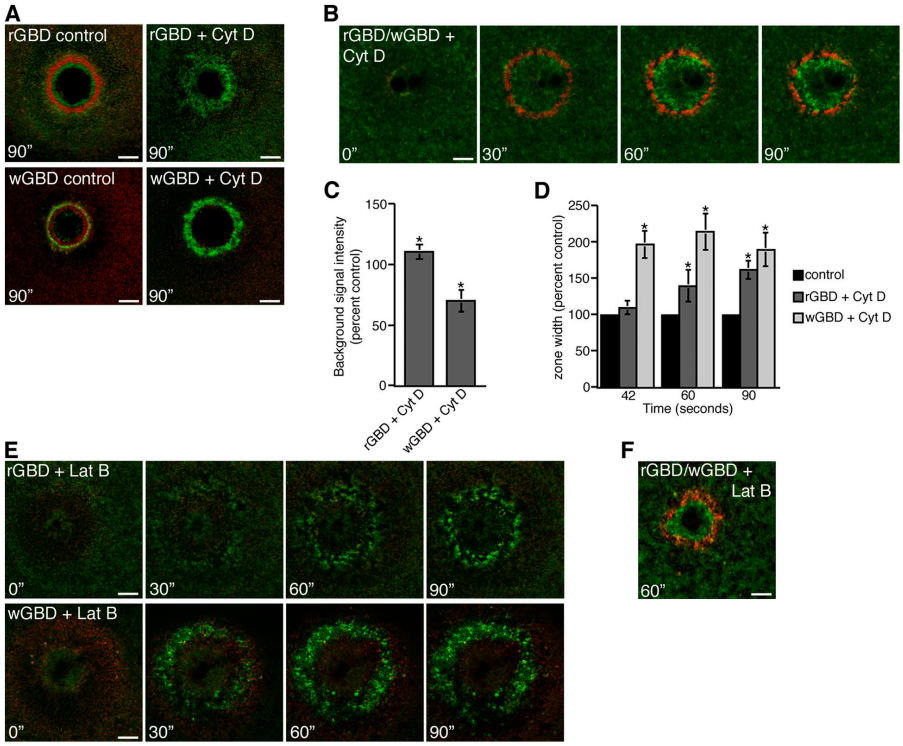

Figure 4. **F-actin and rho GTPase zones.** (A) Montage shows RhoA (rGBD) or Cdc42 (wGBD) activity zones (green) relative to actin (red) in controls and cytochalasin D–treated cells (Cyt D) at 90 s after wounding. Bars, 15 μm. (B) Montage shows that RhoA (rGBD; green) and Cdc42 (wGBD; red) activity zones appear and segregate in the presence of cytochalasin D during wound healing (time in seconds). Bar, 10 μm. (C) Quantification of GBD fluorescence intensity in resting oocytes in the presence of cytochalasin D, relative to controls ($n = 5$; results are shown as means ± SEM; asterisks indicate $P < 0.05$). (D) Quantification of GBD zone width over time in the presence of cytochalasin D, relative to controls (width refers to the distance from the outer edge of the zone to the inner edge; $n = 7$; results are shown as means ± SEM; asterisks indicate $P < 0.05$). (E) Montage shows activity zones of RhoA (rGBD) or Cdc42 (wGBD; green) relative to actin (red), in the presence of latrunculin B (Lat B), during wound healing (time in seconds). Bars, 10 μm. (F) Confocal image shows activity zones of RhoA (green) and Cdc42 (red) 60 s after wounding in the presence of latrunculin B. Bar, 10 μm.

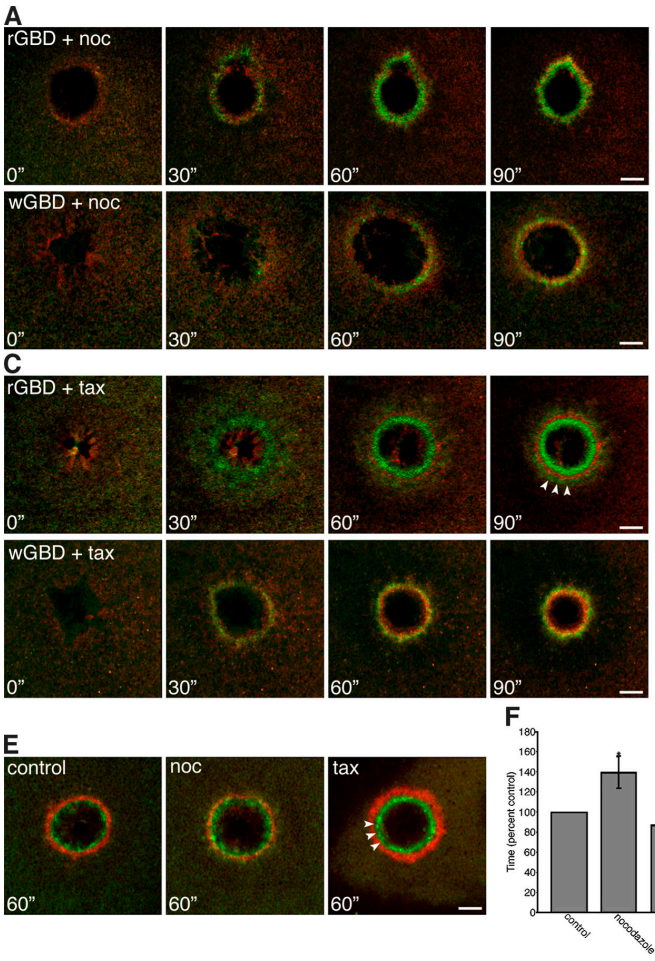

Figure 5. **Microtubules and rho GTPase activation.** (A) Montage shows the broadening of RhoA (rGBD) or Cdc42 (wGBD; green) activity relative to actin (red) in cells treated with nocodazole (noc; time in seconds). Bars, 10 μm. (B) Quantification of GBD zone width over time in the presence of nocodazole, relative to controls ($n = 3$; results are shown as means ± SEM; asterisks indicate $P < 0.05$). (C) Montage shows the broadening of RhoA (rGBD) or Cdc42 (wGBD; green) activity zones relative to actin (red) in cells treated with taxol (tax; arrowheads show rGBD signal on the outside of the actin array; time in seconds). Bars, 10 μm. (D) Quantification of GBD zone width over time in the presence of taxol, relative to controls ($n = 3$; results are shown as means ± SEM; asterisks indicate $P < 0.05$). (E) Montage shows the segregation of RhoA (rGBD; green) and Cdc42 (wGBD; red) activity zones at 60 s after wounding in control and nocodazole- and taxol-treated cells (arrowheads show gap between zones in taxol). Bar, 10 μm. (F) Quantification of the time needed for GBD zone segregation in the presence of nocodazole or taxol, compared with controls ($n = 11$; results are shown as means ± SEM; asterisks indicate $P < 0.05$). (G) Quantification of zone segregation, comparing signal ratio (red/green; mRFP-wGBD/eGFP-rGBD) in the red zone, of controls and oocytes treated with nocodazole or taxol ($n = 9$; results are shown as means ± SEM; asterisks indicate $P < 0.05$).

bers of the Cdc42 family (e.g., TC10 or CHP) are also detected by the wGBD probe, but the reportedly limited expression pattern of these proteins (Drivas et al., 1990; Aronheim et al., 1998; Neudauer et al., 1998) renders this possibility unlikely.

Calcium and local GTPase activation

The immediate consequence of cell wounding is an inrush of external calcium, which triggers rapid (within seconds) fusion of cellular membrane compartments that patch the damaged PM (for review see McNeil and Steinhardt, 2003). So that we could assess the importance of external calcium for RhoA and Cdc42 activation, oocytes were washed with and then wounded in calcium-free medium. This resulted in a nearly complete suppression of RhoA and Cdc42 activation (Fig. 3). A lack of external calcium also prevented accumulation of actin and cortical flow (not depicted, but see Bement et al., 1999). Thus, external calcium is required for local activation of RhoA and Cdc42.

Contributions of the actin cytoskeleton

Disruption of F-actin before wounding does not prevent recruitment of myosin-2 or upstream regulators of actin assembly (Bement et al., 1999; Mandato and Bement, 2001). To determine if the zones of RhoA and Cdc42 activity likewise form after F-actin disruption, we treated oocytes with cytochalasin D before wounding. Concentrations of cytochalasin D sufficient to completely suppress actomyosin-based flow toward wounds (not depicted) failed to prevent formation of RhoA and Cdc42 activity zones around wounds (Fig. 4, A and B). Furthermore, RhoA activity was highest inside the remnants of the actin cytoskeleton at the edge of wounds, whereas Cdc42 activity was highest in the region overlapping the remnants of actin, farther from the wound edge, suggesting that the two zones segregated properly (Fig. 4 A). This point was confirmed when oocytes expressing eGFP-rGBD and mRFP-wGBD were wounded in the presence of cytochalasin (Fig. 4 B). Although cytochalasin did not prevent RhoA and Cdc42 activation or segregation, it elevated resting levels of RhoA activity and reduced resting levels of Cdc42 activity (Fig. 4 C). Cytochalasin also prevented inward movement of the zones of RhoA and Cdc42 activity and increased the width of both activity zones (Fig. 4, B and D).

As an alternative means of disrupting the actin cytoskeleton, latrunculin B was used. After wounding, latrunculin-treated oocytes formed broad zones of RhoA and Cdc42 activity that segregated but failed to move forward (Fig. 4, E and F), which is similar to results obtained with cytochalasin. Thus, the actin cytoskeleton is required for GTPase activity zone translocation and proper concentration of active RhoA and Cdc42 into narrow zones, but is not required for zone formation or segregation.

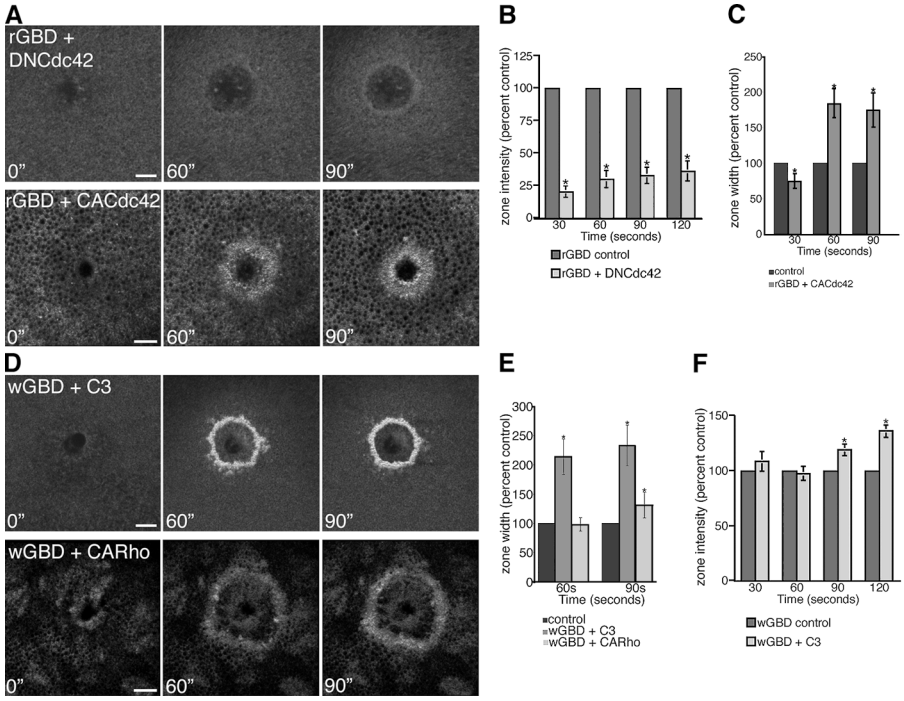

Figure 6. **Crosstalk and rho GTPase zones.** (A) Montage shows a decrease in RhoA activity zone intensity (rGBD) in the presence of DNCdc42 and an increase in zone width in the presence of CACdc42 (time in seconds). Bars, 10 μm. (B) Quantification of rGBD zone fluorescence intensity over time in the presence of DNCdc42 relative to controls ($n = 8$; results are shown as means ± SEM; asterisks indicate $P < 0.05$). (C) Quantification of rGBD zone width over time in the presence of CACdc42, relative to controls ($n = 11$; results are shown as means ± SEM; asterisks indicate $P < 0.05$). (D) Montage shows an increase in Cdc42 activity zone intensity (wGBD) in the presence of C3 and an increase in zone width with both C3 and CARho (time in seconds). Bars, 10 μm. (E) Quantification of wGBD zone signal width over time in the presence of C3 or CARho, relative to controls ($n \geq 4$; results are shown as means ± SEM; asterisks indicate $P < 0.05$). (F) Quantification of wGBD zone fluorescence intensity over time in the presence of C3, relative to controls ($n = 8$; results are shown as means ± SEM; asterisks indicate $P < 0.05$).

Contributions of the microtubule cytoskeleton

Microtubules modulate the actomyosin array that forms around wounds (Mandato and Bement, 2003). To assess the role of microtubules in the RhoA and Cdc42 zones, we first wounded oocytes after treating them with nocodazole, a microtubule-destabilizing drug. Nocodazole did not prevent activation of RhoA or Cdc42 around wounds, nor did it prevent translocation of the activity zones (Fig. 5 A). However, comparison of the distributions of active RhoA or Cdc42 and actin revealed that nocodazole often resulted in broader, more irregular zones (Fig. 5, A and B). Furthermore, direct comparison of rGBD and wGBD in nocodazole-treated oocytes revealed that segregation was significantly inhibited (Fig. 5, E–G).

As an alternative approach, oocytes were wounded after taxol treatment, which increases total microtubule levels (Canman and Bement, 1997). Taxol broadened the activity zones (Fig. 5, C and D) and, by later time points, sometimes split the RhoA activity zone such that it was found on the outside of the actin array (Fig. 5 C, arrowheads). Comparison of rGBD and wGBD distribution in taxol-treated oocytes revealed that taxol promoted zone segregation and sharpened the boundaries between the activity zones such that a narrow, but distinct, gap between rGBD and wGBD signal was apparent (Fig. 5 E, arrowheads) and the wGBD to rGBD signal ratio was increased (Fig. 5 G). Furthermore, taxol decreased the time it took for the activity zones to segregate (Fig. 5 F). Thus, microtubules positively regulate zone segregation but are not required for zone formation or translocation.

Contributions of crosstalk

Rho GTPases can modulate each other's activity in a variety of contexts (Li et al., 2002). By examining the effects of either DN- or CACdc42 on rGBD distribution, we assessed potential crosstalk between RhoA and Cdc42. DNCdc42 almost completely eliminated local RhoA activation after wounding (Fig. 6, A and B). In contrast, CACdc42, which elevates background levels of Cdc42 activity but eliminates the Cdc42 activity zone, significantly broadened the zone of RhoA activity (Fig. 6, A and C). Thus, Cdc42 may both positively and negatively regulate RhoA activation (see Discussion).

In reciprocal experiments, the effects of C3 or CARho on wGBD distribution were determined. C3, which eliminates the RhoA zone, resulted in broadening and elevation of Cdc42 zone signal intensity (Fig. 6, D–F). CARho, which narrows the RhoA zone, also broadened the Cdc42 zone, although to a lesser degree than C3 (Fig. 6, D and E). Thus, although the same general effect (Cdc42 zone broadening) results from essentially opposite treatments (C3 and CARho), the results are consistent with a mechanism in which RhoA locally antagonizes Cdc42 (see Discussion).

Rho GTPase activity zones control specific features of the actomyosin array

To determine whether the rho GTPase activity zones control the actomyosin array elicited by wounding, we first compared the distribution of rGBD with that of activated (ser19 phosphorylated) myosin-2 regulatory light chain (P-MLC), a downstream RhoA target (Amano et al., 1996; Kimura et al., 1996). P-MLC concentrated in a tight ring on the interior of the wGBD zone, in the region of high RhoA activity (Fig. 7 A). In oocytes expressing CACdc42, which eliminates the Cdc42 activity zone and broadens that of RhoA, the distribution of P-MLC was also broadened (Fig. 7 B). Furthermore, inhibition of RhoA using C3 virtually eliminated P-MLC accumulation (Fig. 7 B). Thus, the activity zones direct local asymmetries in downstream targets.

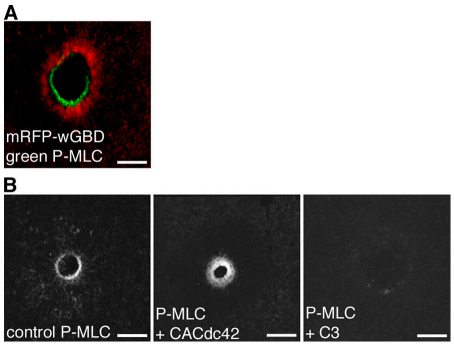

Figure 7. **Activity zones and myosin-2 light chain phosphorylation.** (A) Confocal image shows phosphorylated myosin-2 regulatory light chain staining (P-MLC; green) circumscribed by Cdc42 activity (red) in a fixed cell. Bar, 25 μm. (B) Confocal images of fixed cells show that P-MLC staining is broadened in cells treated with CACdc42 and reduced with C3, compared with control, at 3 min after wounding. Bars, 25 μm.

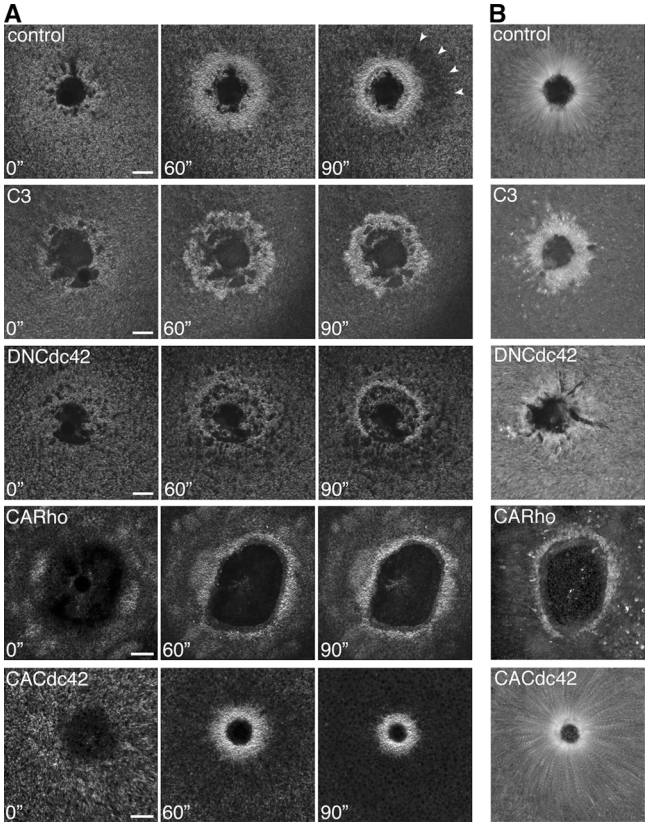

Figure 8. **Contributions of rho GTPases to actin assembly and closure.** (A) Montage shows varied appearance and dynamics of actin in cells treated with either C3, DNCdc42, CARho, or CACdc42, compared with control (arrowheads indicate the outer edge of the dark halo in control). Bars, 15 μm. (B) Montage of brightest point projections made from movies (available at http://www.jcb.org/cgi/content/full/jcb.200411109/DC1) shows that movement of individual actin filament clusters around wounds is greatly reduced in cells treated with C3, DNCdc42, or CARho, but increased with CACdc42, compared with control. Videos available at http://www.jcb.org/cgi/content/full/jcb.200411109/DC1.

The effects of C3, DNCdc42, CARho, or CACdc42 on the dynamics of the actin array were then monitored. In control cells, actin rapidly accumulated in a circular array around wounds (Fig. 8 A). This array then moved inward, accompanied by actomyosin-based cortical flow, which was revealed by a dark halo of F-actin depletion around it (Fig. 8 A, arrowheads; and Video 6; Mandato and Bement, 2001). This translocation of F-actin can be easily visualized by brightest point projections of multiple time points, which show directed movement of individual F-actin aggregates from the surrounding cortex to the wound border as continuous linear arrays that radiate outward from the wound (Fig. 8 B). C3 almost completely suppressed cortical flow, as shown by the lack of a dark halo and a lack of directed movement in the brightest point projections (Fig. 8, A and B, and Video 7). However, C3 did not prevent local actin assembly around wounds, as revealed by the accumulation of actin around wounds in movies and the appearance of isolated, actin-rich structures in brightest point projections, which is consistent with its observed effect of increasing local Cdc42 activation around wounds. DNCdc42, in contrast, reduced local actin accumulation as well as cortical flow (Fig. 8, A and B, and Video 8), in keeping with the observation that it prevents RhoA zone formation. CARho expression, which elevates background levels of RhoA activity while inhibiting the RhoA activity zone, resulted in a global contraction of the oocyte cortex even before wounding, as judged by increased cortical stiffness and accumulation of pigment granules into discrete islands throughout the cortex (unpublished data). Upon wounding, oocytes expressing CARho displayed large wounds, which is consistent with a cortex under tension, and sharply reduced cortical flow and disorganized actin assembly (Fig. 8, A and B, and Video 9). The actin arrays thus formed frequently broke, as if trying (and failing) to contract inward against globally elevated contractility (unpublished data). CACdc42, which prevents Cdc42 activity zone formation and enhances the RhoA activity zone, on the other hand, greatly accelerated cortical flow and increased the distance from the wound edge affected by flow (Fig. 8, A and B, and Video 10). Thus, Cdc42 positively regulates both local actin assembly and contractility (with the latter activity presumably resulting from its positive regulation of RhoA), whereas RhoA positively regulates contractility and negatively regulates actin assembly (with the latter activity presumably resulting from its negative regulation of Cdc42).

Discussion

This study reveals the existence of mobile, concentric, sharply bounded zones of RhoA and Cdc42 activity that form in response to cellular wounding. The formation, segregation, and translocation of these activity zones are regulated by inputs from external calcium, the actin cytoskeleton, microtubules, and crosstalk between RhoA and Cdc42. Furthermore, these zones make distinct functional contributions to the actomyosin array around wounds. As described in the following paragraphs, these findings not only explain previous results from the oocyte wound healing system, but they also provide important insights into other processes requiring coordination of actin assembly and actomyosin-based contraction.

The existence and characteristics of the RhoA and Cdc42 activity zones explain three intriguing features of wound-

induced actomyosin arrays. First, regulators of actin assembly and myosin-2 accumulate around wounds even when the actin cytoskeleton is disrupted, as do the RhoA and Cdc42 zones. This affirms the proposal that the actomyosin array must be underlaid by localized signals that operate independently of the F-actin cytoskeleton (Bement et al., 1999; Mandato and Bement, 2001) and identifies RhoA and Cdc42 as two of the hypothesized signaling proteins. Second, the wound-induced actomyosin array segregates over time, such that myosin-2 becomes concentrated on the inside of the array, whereas dynamic actin is concentrated on the outside of the array (Bement et al., 1999; Mandato and Bement, 2001). The segregation of the RhoA and Cdc42 activity zones precisely parallels this finding, and the effects of zone disruption on both the dynamics of the actin array and the distribution of P-MLC show that zone segregation is required for functional segregation of the actomyosin array. Third, microtubules control the organization of the actomyosin array (Mandato and Bement, 2003) and, similarly, the organization and segregation of the RhoA and Cdc42 activity zones. Therefore, we conclude that the zones of active RhoA and Cdc42 are responsible for many of the basic features of the wound-induced actomyosin array.

What triggers activation of rho GTPases? Our results indicate that calcium is an essential upstream trigger. In other systems, PM damage triggers rapid, calcium-dependent membrane fusion that patches the damaged area (for review see McNeil and Steinhardt, 2003). Thus, both early (membrane patching) and late (rho GTPase activation) events resulting from wounding stem from the same upstream trigger. Curiously, the ~20 s required for RhoA and Cdc42 activation is more time than the few seconds required for the patching event (Steinhardt et al., 1994). This latent period, and the absence of any reports of direct effects of calcium on RhoA and Cdc42, indicate that several steps intervene between calcium elevation and rho GTPase activation. The nature of these steps is unknown; however, wounding results in local exocytosis (Steinhardt et al., 1994), and calcium-dependent exocytosis of *Xenopus* egg cortical granules triggers Cdc42 activation after a delay of ~12 s (Sokac et al., 2003), which suggests that GTPase activation could result from exocytosis.

The demonstration that cellular damage is coupled to RhoA and Cdc42 activation via calcium is of considerable importance for tissue wounds, as well, because RhoA (Brock et al., 1996) and Cdc42 (Fenteany et al., 2000) participate in multicellular wound healing, and because such wounding typically results in PM disruption (and presumptive calcium elevation) in wound border cells (Brock et al., 1996). Furthermore, both actin assembly (Miyake et al., 2001) and myosin-2 (Togo and Steinhardt, 2004) have been implicated in single cell wound healing in cultured mammalian cells. Therefore, it will be of great interest to determine if local rho GTPase activation is a general feature of the wound response.

Even more striking than activation of RhoA and Cdc42 around wounds is the characteristically precise, dynamic organization of the activity zones into mobile, discrete concentric rings. Both zones form before the onset of actin accumulation and cortical flow, and both translocate in concert with actin

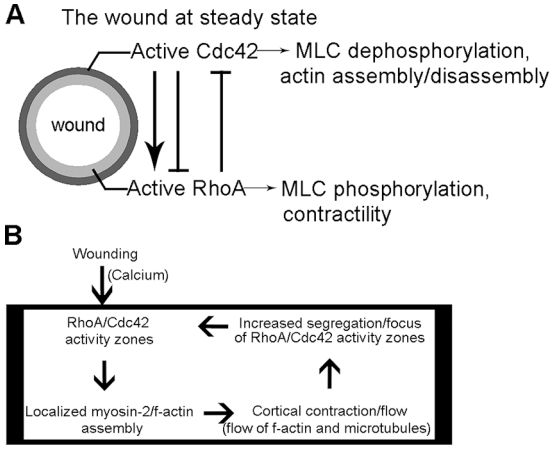

Figure 9. **Summary, crosstalk, and working model for observed discrete localization of rho GTPase activity zones during wound healing.** (A) Schematic shows observed concentric subcellular compartmentalization of RhoA and Cdc42 activity zones at wound border, summary of crosstalk, and their respective effects on actin dynamics. (B) Diagram shows working model for maintenance of wound-induced response. Upon wounding, a cytoplasmic activity module (inside box) is established in which activation of localized RhoA and Cdc42 leads to directed cortical contraction and flow, which cause accumulation of both actin and microtubules, which, in turn, further promotes zones of activity.

array closure. Although it is generally assumed that different rho GTPases are active in different subcellular regions, and visualization of individual GTPases supports this notion (Introduction), this work provides the first direct demonstration of such subcellular partitioning in single, living cells. The concentric organization of the activity zones, and the results of zone perturbation on MLC phosphorylation and actin dynamics, suggest a functional rationale for the segregation of the activity zones (Fig. 9 A). Specifically, we propose that concentration of RhoA activity on the interior of the cytoskeletal array ensures that MLC phosphorylation, and, therefore, myosin-2 activity, remain high in this region. Conversely, concentration of Cdc42 activity on the exterior of the cytoskeletal array directs actin assembly/disassembly in this region. It would also be expected to promote MLC dephosphorylation, via activation of Pak1 (Sanders et al., 1999). Thus, the concentric organization of the activity zones ensures that a region of high contractility is followed by one of low contractility. This organization would ensure that myosin-2–dependent contraction is not futilely expended fighting contraction outside the wound region, as was observed in the CARho expression experiments. It could also ensure at later stages in the wound healing process that myosin-2 is disassembled in a timely fashion, as is suggested by the accumulation of P-MLC observed in CACdc42 expression experiments.

The organization and translocation of the activity zones is controlled at least in part by the cytoskeleton. F-actin is not required for the formation or segregation of the two zones, but is required for focusing active RhoA and Cdc42 into tight zones, and for proper zone translocation. The almost complete abolishment of zone translocation and the decrease in zone focus of active RhoA and Cdc42 after F-actin disruption indicate that F-actin provides a mobile scaffold required for proper distribution of the active GTPases, as suggested previously (Mandato

and Bement, 2001). Microtubules are dispensable for zone formation and translocation, but are required for proper zone organization and segregation. What exerts this control is unknown, but microtubule-binding rho GTPase regulatory proteins are obvious choices (Krendel et al., 2002).

GTPase crosstalk is important for both zone formation and organization. Specifically, RhoA negatively modulates the Cdc42 activity zone (Fig. 9 A), based on exclusion of active Cdc42 from the RhoA zone and the fact that manipulations, which eliminate or reduce the RhoA zone, result in a corresponding increase in the size of the Cdc42 zone. This implies that at least some aspects of zone segregation may be autonomous, such that initially overlapping regions of RhoA and Cdc42 activity could self-sort into distinct domains. Conversely, inhibition of Cdc42 activity strongly suppresses local RhoA activation. This result is paradoxical, in that RhoA activity is largely excluded from the Cdc42 activity zone, and elimination of the Cdc42 activity zone by expression of CACdc42 broadens the RhoA activity zone. Therefore, we propose that although some minimal amount of Cdc42 activity is required for RhoA activation, the high level of Cdc42 activity in the zone locally antagonizes RhoA activity (Fig. 9 A).

Besides providing insight into crosstalk between RhoA and Cdc42, the constitutively active probes also provide surprising insights into potential means by which the zones themselves form. That is, we found complete suppression of the Cdc42 zone by CACdc42 and reduction in the RhoA zone by CARho, even though the endogenous, wild-type GTPases were still present. We can envision three potential explanations for these results. First, the long-term presence of the constitutively active GTPases might perturb some feature of the cortex that is required for normal zone formation. If so, it is unlikely to be simple disruption of the cortical cytoskeleton, because zone formation is not prevented by cytochalasin, latrunculin, or nocodazole. Second, high background levels of rho GTPase activity may tie up factors required for activation of the GTPases at the wound border. For example, it has recently been shown that the Rac/Cdc42 effector, Pak1, participates in a feed forward loop in which active Pak1 phosphorylates rho GDI, thereby specifically inhibiting the interaction of rho GDI with Rac1 and, thus, promoting Rac1 activation (DerMardirossian et al., 2004). Third, the formation and maintenance of the activity zone may require Cdc42 activity turnover, a possibility consistent with the notion that rho GAPs may be required for positive aspects of rho GTPase activity (for review see Bernards and Settleman, 2004).

The characteristics of the RhoA and Cdc42 activity zones fulfill one of the major predictions of the cytoplasmic activity module hypothesis, which was developed to explain how the actin and microtubule cytoskeletons are integrated to control complex motility processes (Rodriguez et al., 2003). In brief, it was envisioned that overlapping contributions from actomyosin and microtubules facilitate the formation and segregation of mobile regions of rho GTPase activity, which, in turn, feed back into maintenance and direction of cytoskeleton polarization. As is described in the present study, microtubules and actin promote normal segregation and organization of the rho GTPase activity zones, and the zones clearly contribute to the functional polarization of the cytoskeleton. These results, when considered with previous findings (Mandato and Bement, 2001, 2003), suggest a working model in which a cytoplasmic activity module is generated by wound-induced activation of RhoA and Cdc42, leading to local assembly of myosin-2 and F-actin (Fig. 9 B). The resultant accumulation of F-actin and active myosin-2 then results in cortical contraction and flow, bringing with it microtubules physically linked to other microtubules (Mandato and Bement, 2003) and more F-actin (Mandato and Bement, 2001). Microtubule and actomyosin recruitment, in turn, promote focusing and segregation of the rho GTPase activity zones, which further promotes cortical contraction and flow and so on.

Whether mobile, segregated zones of rho GTPase activity are harnessed in other cellular contexts remains to be seen, although it is clear that rho GTPase activity is highly polarized in locomoting cells (Xu et al., 2003; Nalbant et al., 2004). Furthermore, preliminary studies indicate that cytokinesis is accompanied by the formation of precisely bounded, microtubule-dependent rho GTPase activity zones in the furrow region (unpublished data), which is consistent with previous suggestions (Mandato et al., 2000). Therefore, we speculate that complementary rho GTPase activity zones are likely to be used in a variety of situations in which local contractility and actin assembly require tight coordination. Two other obvious examples are cell cycle–entrained contraction and relaxation (Hara et al., 1980) and morphogenetic processes such as dorsal closure in *Drosophila* (for review see Harden, 2002). The approach described in this study has considerable promise for testing these possibilities.

Materials and methods

Preparation of probes

GST-rGBD (provided by K. Burridge, The University of North Carolina at Chapel Hill, Chapel Hill, NC) was bacterially expressed and purified on glutathione-Sepharose beads (Amersham Biosciences), eluted, and frozen in liquid N_2 at 2 mg/ml. eGFP-rGBD, eGFP-wGBD, and mRFP-wGBD constructs were amplified from pGEX constructs (GST-wGBD was provided by H. Higgs, Dartmouth Medical School, Hanover, NH), cloned into a custom pCS2-eGFP vector (Sokac et al., 2003) or pCS2-mRFP (mRFP provided by R. Tsien, University of California, San Diego, La Jolla, CA; Campbell et al., 2002), and transcribed in vitro using the mMessage mMachine SP6 kit (Ambion). CACdc42, CARho, DNCdc42, and wild-type Cdc42 constructs (provided by T. Gomez, The University of Wisconsin–Madison, Madison, WI) were transcribed in vitro.

Acquisition, microinjection, and manipulation of oocytes

Oocytes were obtained from adult females, defolliculated, and stored in 1× OR2 (82.5 mM NaCl, 2.5 mM KCl, 1 mM $CaCl_2$, 1 mM $MgCl_2$, 1 mM Na_2HPO_4, and 5 mM Hepes, pH 7.4) containing 5 mg/ml BSA. All injections were done using glass needles having a bore size of ~5 μm in diameter attached to a Pico-Injector (model PLI-100; Medical Systems Corp.), and oocytes receiving multiple injections were allowed 1 h to recover between injections. Purified GST-rGBD was diluted in water and injected into oocytes to a final concentration of 20 μg/ml 2 h before wounding. rGBD- and wGBD-encoding mRNAs were injected into oocytes to a final concentration of ~27 μg/ml and 20 μg/ml, respectively, 24 h before wounding. Concentrations three times greater than these inhibited the healing process, presumably because the probes compete for binding to the active GTPases with endogenous effectors (Fig. S3, available at http://www.jcb.org/cgi/content/full/jcb.200411109/DC1). Constitutively active and dominant negative RNAs were injected into oocytes to a final concentration of 80 μg/ml 48 h before wounding. Alexa 568 and 488 G-actin (Molecular Probes) were injected to a final concentration of 6

μg/ml 24 h before wounding. GTP-γ-S (in water) was injected to a final concentration of 5 mM. C3 exotransferase (Cytoskeleton, Inc.) and toxin B (Calbiochem) were injected to final concentrations of 0.08 μg/μl and 2 ng/μl, respectively, 2–4 h before wounding. Cytochalasin D and latrunculin B were applied at final external concentrations of 20 μM and 10 μM, respectively, for 1 h before wounding. Nocodazole and taxol were applied at final external concentrations of 40 μM and 20 μM, respectively, 1 h before wounding. Laser wounds were made using a Micropoint pulse nitrogen-pumped dye laser (Laser Science, Inc.) through a 25× objective in fixed experiments, and through a 60× objective in live experiments. (The laser heats up the pigment granules, causing them to explode and tear a hole in the cell surface. In many wounds, what appears to be a gas bubble also forms at the site of laser damage. As this bubble escapes from the cell, cytoplasm fills in behind it, giving the impression of a second wound healing rapidly inside the first.) In fixed experiments, oocytes were allowed to heal for 2–5 min and fixed overnight (ON) in a 10-mM EGTA, 100-mM KCl, 3-mM $MgCl_2$, 10-mM Hepes, and 150-mM sucrose buffer at pH 7.6, containing 4% PFA, 0.1% gluteraldehyde, and 0.1% Triton X-100. Oocytes were then washed several times in 1×PBS, quenched for 4 h in 1×PBS containing 100 mM sodium borohydride, washed several times in TBSN/BSA (5 mg/ml BSA in 1×TBS containing 0.1% NP-40), bisected, and washed ON at 4°C.

Staining, confocal microscopy, and analyses of wounds

Fixed samples were stained ON with TR phalloidin (Molecular Probes) at 1:100 and goat anti-GST (Amersham Biosciences) at 1:1,000 or anti–P-MLC (Cell Signaling Technology) at 1:100, in TBSN/BSA at 4°C. Cells were then washed for 24 h, incubated ON at 4°C in Alexa 488 rabbit anti–goat at 1:250 or a mixture of anti–Rab-Cy5 and Fab anti–Rab-Cy5 at 1:200, washed for 24 h, mounted on slides and viewed using a 1.4-NA 63× objective. All imaging was done using an Axiovert 100M (Carl Zeiss MicroImaging, Inc.) with the Lasersharp Confocal package (model 1024; Bio-Rad). Image analyses were done using NIH Object Image v2.06, Adobe Photoshop 3.0 and 7.0, and Volocity 2.0.1. Brightest point projections were made from 4D confocal movies; each frame of each movie was projected onto the next such that one projection displays movement seen in an entire movie sequence. Statistical analyses were performed using Microsoft Excel, and graphs were generated.

Online supplemental material

10 videos are included as 4D movies depicting the dynamics of RhoA activity, Cdc42 activity, and actin during wound healing. Videos 1–5 complement the images in Fig. 2, showing the dynamics of RhoA activity and Cdc42 activity either relative to actin, alone, or relative to one another during wound healing. Videos 6–10 complement Fig. 8, showing 4D movies of actin dynamics during wound healing in control oocytes, oocytes in which RhoA is inhibited or promoted, and oocytes in which Cdc42 activity is inhibited or promoted. Three supplemental figures are also included. Fig. S1 (A and B) further confirms RhoA and Cdc42 activity zone localization relative to actin, and Fig. S1 C provides chymographs depicting zone dynamics. Fig. S2 shows that the zone of Cdc42 activity localizes within the total Cdc42 at the wound border. Fig. S3 confirms that overexpression of wGBD probe inhibits wound healing. Online supplemental material is available at http://www.jcb.org/cgi/content/full/jcb.200411109/DC1.

This paper is dedicated to the memory of Warren Zevon.

We would like to thank C. Mandato, A. Sokac, and H.-Y. Yu for sharing ideas, expertise, and/or materials. Thanks to K. Burridge, H. Higgs, T. Gomez, and R. Tsien for sharing constructs, and to our current lab members for support and encouragement.

The National Institutes of Health (grant GM52932-04A1) and the National Science Foundation (NSF; grant MCB9630860) supported this work. The NSF supported the acquisition of the confocal microscope used in this study (grant NSF9724515 to J. Pawley).

Submitted: 18 November 2004
Accepted: 13 December 2004

References

Aktories, K., C. Wilde, and M. Vogelsgesang. 2004. Rho-modifying C3-like ADP-ribosyltransferases. *Rev. Physiol. Biochem. Pharmacol.* 152:1–22.

Amano, M., M. Ito, K. Kimura, Y. Fukata, K. Chihara, T. Nakano, Y. Matsuura, and K. Kaibuchi. 1996. Phosphorylation and activation of myosin by Rho-associated kinase (Rho-kinase). *J. Biol. Chem.* 271:20246–20249.

Aronheim, A., Y.C. Broder, A. Cohen, A. Fritsch, B. Belisle, and A. Abo. 1998. Chp, a homologue of the GTPase Cdc42Hs, activates the JNK pathway and is implicated in reorganizing the actin cytoskeleton. *Curr. Biol.* 8:1125–1128.

Bement, W.M., C.A. Mandato, and M.N. Kirsch. 1999. Wound-induced assembly and closure of an actomyosin purse string in *Xenopus* oocytes. *Curr. Biol.* 9:579–587.

Bement, W.M., A.M. Sokac, and C.A. Mandato. 2003. Four-dimensional imaging of cytoskeletal dynamics in *Xenopus* oocytes and eggs. *Differentiation.* 71:518–527.

Bernards, A., and J. Settleman. 2004. GAP control: regulating the regulators of small GTPases. *Trends Cell Biol.* 14:377–385.

Bishop, A.L., and A. Hall. 2000. Rho GTPases and their effector proteins. *Biochem. J.* 348:241–255.

Brock, J., K. Midwinter, J. Lewis, and P. Martin. 1996. Healing of incisional wounds on the embryonic chick wing bud: characterization of the actin purse-string and demonstration of a requirement for Rho activation. *J. Cell Biol.* 135:1097–1107.

Campbell, R.E., O. Tour, A.E. Palmer, P.A. Steinbach, G.S. Baird, D.A. Zacharias, and R.Y. Tsien. 2002. A monomeric red fluorescent protein. *Proc. Natl. Acad. Sci. USA.* 99:7877–7882.

Canman, J.C., and W.M. Bement. 1997. Microtubules suppress actomyosin-based cortical flow in *Xenopus* oocytes. *J. Cell Sci.* 110:1907–1917.

DerMardirossian, C., A. Schnelzer, and G.M. Bokoch. 2004. Phosphorylation of RhoGDI by Pak1 mediates dissociation of Rac GTPase. *Mol. Cell.* 15:117–127.

Drivas, G.T., A. Shih, E. Coutavas, M.G. Rush, and P. D'Eustachio. 1990. Characterization of four novel ras-like genes expressed in a human teratocarcinoma cell line. *Mol. Cell. Biol.* 10:1793–1798.

Fenteany, G., P.A. Janmey, and T.P. Stossel. 2000. Signaling pathways and cell mechanics involved in wound closure by epithelial cell sheets. *Curr. Biol.* 10:831–838.

Hara, K., P. Tydeman, and M. Kirschner. 1980. A cytoplasmic clock with the same period as the division cycle in *Xenopus* eggs. *Proc. Natl. Acad. Sci. USA.* 77:462–466.

Harden, N. 2002. Signaling pathways directing the movement and fusion of epithelial sheets: lessons from dorsal closure in *Drosophila. Differentiation.* 70:181–203.

Jacinto, A., W. Wood, S. Woolner, C. Hiley, L. Turner, C. Wilson, A. Martinez-Arias, and P. Martin. 2002. Dynamic analysis of actin cable function during *Drosophila* dorsal closure. *Curr. Biol.* 12:1245–1250.

Kim, S.H., Z. Li, and D.B. Sacks. 2000. E-cadherin-mediated cell-cell attachment activates Cdc42. *J. Biol. Chem.* 275:36999–37005.

Kimura, K., M. Ito, M. Amano, K. Chihara, Y. Fukata, M. Nakafuku, B. Yamamori, J. Feng, T. Nakano, K. Okawa, et al. 1996. Regulation of myosin phosphatase by Rho and Rho-associated kinase (Rho-kinase). *Science.* 273:245–248.

Kraynov, V.S., C. Chamberlain, G.M. Bokoch, M.A. Schwartz, S. Slabaugh, and K.M. Hahn. 2000. Localized Rac activation dynamics visualized in living cells. *Science.* 290:333–337.

Krendel, M., F.T. Zenke, and G.M. Bokoch. 2002. Nucleotide exchange factor GEF-H1 mediates crosstalk between microtubules and the actin cytoskeleton. *Nat. Cell Biol.* 4:294–301.

Lauffenburger, D.A., and A.F. Horwitz. 1996. Cell migration: a physically integrated molecular process. *Cell.* 84:359–369.

Li, Z., C.D. Aizenman, and H.T. Kline. 2002. Regulation of Rho GTPases by crosstalk and neuronal activity *in vivo. Neuron.* 33:741–750.

Mandato, C.A., and W.M. Bement. 2001. Contraction and polymerization cooperate to assemble and close actomyosin rings around *Xenopus* oocyte wounds. *J. Cell Biol.* 154:785–797.

Mandato, C.A., and W.M. Bement. 2003. Actomyosin transports microtubules and microtubules control actomyosin recruitment during *Xenopus* oocyte wound healing. *Curr. Biol.* 13:1096–1105.

Mandato, C.A., H.A. Benink, and W.M. Bement. 2000. Microtubule-actomyosin interactions in cortical flow and cytokinesis. *Cell Motil. Cytoskeleton.* 45:87–92.

McNeil, P.L., and R.A. Steinhardt. 2003. Plasma membrane disruption: repair, prevention, adaptation. *Annu. Rev. Cell Dev. Biol.* 19:697–731.

Miyake, K., P.L. McNeil, K. Suzuki, R. Tsunoda, and N. Sugai. 2001. An actin barrier to resealing. *J. Cell Sci.* 114:3487–3494.

Nalbant, P., L. Hodgson, V. Kraynov, A. Toutchkine, and K.M. Hahn. 2004. Activation of endogenous Cdc42 visualized in living cells. *Science.* 305:1615–1619.

Neudauer, C.L., G. Joberty, N. Tatsis, and I.G. Macara. 1998. Distinct cellular effects and interactions of the Rho-family GTPase TC10. *Curr. Biol.* 8:1151–1160.

Pertz, O., and K.M. Hahn. 2004. Designing biosensors for Rho family proteins–deciphering the dynamics of Rho family GTPase activation in living cells. *J. Cell Sci.* 117:1313–1318.

Prehoda, K.E., J.A. Scott, R.D. Mullins, and W.A. Lim. 2000. Integration of multiple signals through cooperative regulation of the N-WASP-Arp2/3 complex. *Science.* 290:801–806.

Ren, X.D., W.B. Kiosses, and M.A. Schwartz. 1999. Regulation of the small GTP-binding protein Rho by cell adhesion and the cytoskeleton. *EMBO J.* 18:578–585.

Ridley, A.J. 2001. Rho GTPases and cell migration. *J. Cell Sci.* 114:2713–2722.

Rodriguez, O.C., A.W. Schaefer, C.A. Mandato, P. Forscher, W.M. Bement, and C.M. Waterman-Storer. 2003. Conserved microtubule-actin interactions in cell movement and morphogenesis. *Nat. Cell Biol.* 5:1–11.

Sanders, L.C., F. Matsumura, G.M. Bokoch, and P. de Lanerolle. 1999. Inhibition of myosin light chain kinase by p21-activated kinase. *Science.* 283:2083–2085.

Schirmer, J., and K. Aktories. 2004. Large clostridial cytotoxins: cellular biology of Rho/Ras-glucosylating toxins. *Biochim. Biophys. Acta.* 1673:66–74.

Sokac, A.M., C. Co, J. Taunton, and W.M. Bement. 2003. Cdc42-dependent actin polymerization during compensatory endocytosis in *Xenopus* eggs. *Nat. Cell Biol.* 5:727–732.

Srinivasan, S., F. Wang, S. Glavas, A. Ott, F. Hofmann, K. Aktories, D. Kalman, and H.R. Bourne. 2003. Rac and Cdc42 play distinct roles in regulating PI(3,4,5)P3 and polarity during neutrophil chemotaxis. *J. Cell Biol.* 160:375–385.

Steinhardt, R.A., G. Bi, and J.M. Alderton. 1994. Cell membrane resealing by a vesicular mechanism similar to neurotransmitter release. *Science.* 263:390–393.

Togo, T., and R.A. Steinhardt. 2004. Nonmuscle myosin IIA and IIB have distinct functions in the exocytosis-dependent process of cell membrane repair. *Mol. Biol. Cell.* 15:688–695.

Waterman-Storer, C.M., and E.D. Salmon. 1999. Positive feedback interactions between microtubule and actin dynamics during cell motility. *Curr. Opin. Cell Biol.* 11:61–67.

Xu, J., F. Wang, A. Van Keymeulen, P. Herzmark, A. Straight, K. Kelly, Y. Takuwa, N. Sugimoto, T. Mitchison, and H.R. Bourne. 2003. Divergent signals and cytoskeletal assemblies regulate self-organizing polarity in neutrophils. *Cell.* 114:201–214.

Yoshizaki, H., Y. Ohba, K. Kurokawa, R.E. Itoh, T. Nakamura, N. Mochizuki, K. Nagashima, and M. Matsuda. 2003. Activity of Rho-family GTPases during cell division as visualized with FRET-based probes. *J. Cell Biol.* 162:223–232.

Yumura, S., and T.Q. Uyeda. 2003. Myosins and cell dynamics in cellular slime molds. *Int. Rev. Cytol.* 224:173–225.